(9)

DNA 3920F

DYNAMIC CALIBRATOR FOR AIRBLAST PRESSURE GAGES TO 10,000 PSI

Artec Associates Incorporated
26046 Eden Landing Road
Hayward, California 94545

27 February 1976

Final Report

CONTRACT No. DNA 001-75-C-0041

THIS WORD SPONSORED BY THE DEFENSE NUCLEAR AGENCY
UNDER RDT&E RMSS CODE B344075464 Y99QAXSD07013 H2590D.

Prepared for

Director
DEFENSE NUCLEAR AGENCY
Washington, D. C. 20305

Destroy this report when it is no longer needed.
Do not return to sender.

UNCLASSIFIED

SECURITY CLASSIFICATION OF THIS PAGE (When Data Entered)

REPORT DOCUMENTATION PAGE		READ INSTRUCTIONS BEFORE COMPLETING FORM
1 REPORT NUMBER: DNA 3920F	2 GOVT ACCESSION NO.	3 RECIPIENT'S CATALOG NUMBER
4 TITLE (and Subtitle): DYNAMIC CALIBRATOR FOR AIRBLAST PRESSURE GAGES TO 10,000 PSI.		5 TYPE OF REPORT & PERIOD COVERED: Final Report.
		6 PERFORMING ORG. REPORT NUMBER: FR-114
7 AUTHOR(s): Stephen P. Gill, Michael B. Gross		8 CONTRACT OR GRANT NUMBER(s): DNA 001-75-C-0041 NEW
9 PERFORMING ORGANIZATION NAME AND ADDRESS: Artec Associates Incorporated, 26046 Eden Landing Road, Hayward, California 94545		10 PROGRAM ELEMENT, PROJECT, TASK AREA & WORK UNIT NUMBERS: NWED Subtask Y99QAXSD070-13
11 CONTROLLING OFFICE NAME AND ADDRESS: Director, Defense Nuclear Agency, Washington, D.C. 20305		12 REPORT DATE: 27 February 1976
		13 NUMBER OF PAGES: 58
14 MONITORING AGENCY NAME & ADDRESS (if different from Controlling Office): DNH-NWED-QHXS		15 SECURITY CLASS (of this report): UNCLASSIFIED
		15a DECLASSIFICATION/DOWNGRADING SCHEDULE

16 DISTRIBUTION STATEMENT (of this Report)

Approved for public release; distribution unlimited.

17 DISTRIBUTION STATEMENT (of the abstract entered in Block 20, if different from Report)

18 SUPPLEMENTARY NOTES

This work sponsored by the Defense Nuclear Agency under RDT&E RMSS Code B344075464 Y99QAXSD07013 H2590D.

19 KEY WORDS (Continue on reverse side if necessary and identify by block number)

Calibration
Airblast Measurements
Pressure Gage

20 ABSTRACT (Continue on reverse side if necessary and identify by block number)

A compact inverted shock tube concept is recommended for a field-portable airblast pressure gage calibrator in the pressure range 100 - 10,000 psi. This concept meets all operational and performance specifications agreed upon by DNA and the user community.

DD FORM 1 JAN 73 1473 EDITION OF 1 NOV 65 IS OBSOLETE

UNCLASSIFIED

SECURITY CLASSIFICATION OF THIS PAGE (When Data Entered)

408296

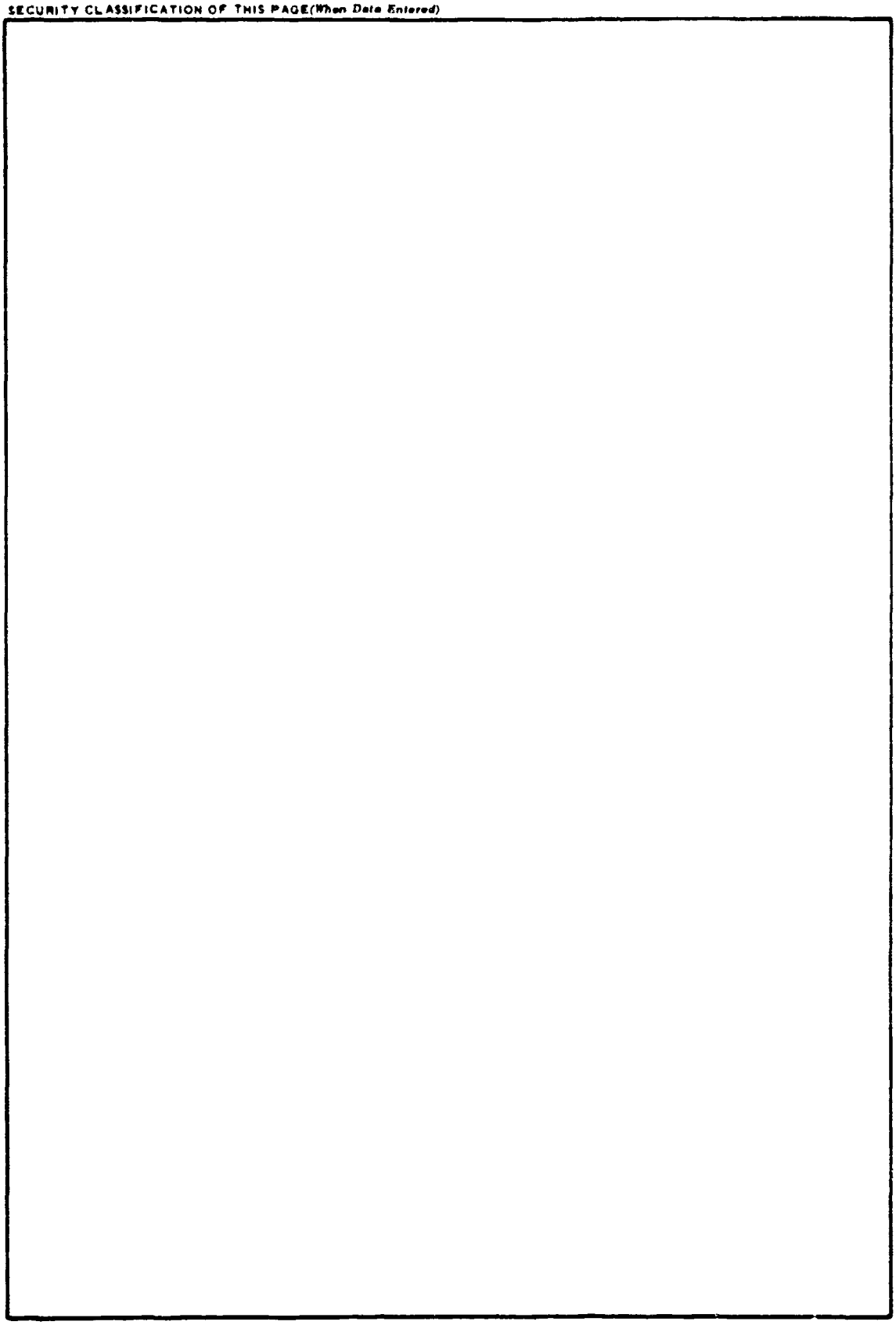

CONTENTS

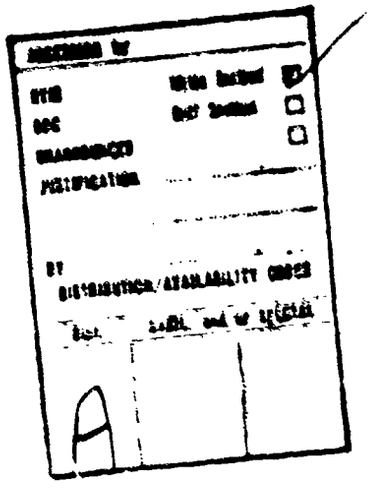

ILLUSTRATIONS

TABLES

1. INTRODUCTION

Technology advances in nuclear-hardened military systems have introduced requirements for airblast testing of components and systems to very high overpressure levels. Measurement and interpretation of high overpressure data gathered on large high explosive tests conducted by DNA continues to pose technical problems; particularly troublesome is the fact that individual blast overpressure measurements have varied by as much as a factor of two when different gages and recording systems are used. As the cost per data channel continues to increase, it has become highly desireable to provide a uniform standard of field calibration at high overpressure levels to assure proper functioning of gages and recording systems immediately prior to a test.

No field portable calibration system now exists capable of testing fast-response blast gages in the 1000 to 10,000 psi overpressure range. Quasi-static (rise time of several milliseconds) calibration techniques are in common use at lower overpressures (Reference 1), and in some cases these techniques could be extended to high overpressures. However, since the risetime to peak pressure in actual measurements is on the order of microseconds, there is serious doubt as to the adequacy of quasi-static techniques for field calibration purposes.

The purpose of the present program was to review the

entire spectrum of pressure gage calibration system concepts, and to recommend a calibration system for DNA field use at blast overpressures from 100 to 10,000 psi. The first part of the study involved the determination of reasonable performance specifications and operational requirements acceptable to the user community; the remainder of the program concentrated on technical innovations and engineering design to meet these specifications.

2. DESIGN CRITERIA

Design criteria for the high pressure field calibrator system were developed only after considerable debate with DNA and the user community. It was at first envisioned that the calibrator would directly simulate aspects of the environment known to affect gages at high overpressures, namely high temperatures and high dynamic pressures. Although it is possible to generate the desired environments with a number of high energy simulation concepts, their complexity, size, and cost are entirely unsuited for field calibration purposes. Conflict between an ideal laboratory environment simulator and a practical cost-effective dynamic calibrator for field use was decided by DNA in favor of the latter for the present design study.

Performance and operational system design criteria were established jointly with DNA. The performance criteria are:

1. Overpressure range 100 - 10,000 psi.
2. Repeatable within 5%.
3. Pressure pulse of sufficient duration to allow for gage equilibration.
4. Pulse will have a fast-rising leading edge.

The fourth requirement is tentative, depending on system frequency response and whether peak overpressure or impulse is to be determined.

Operational system criteria are as follows:

1. Safe for nearby personnel and equipment, with no personnel evacuation during a test.
2. Truck portable.
3. Inexpensive to operate.
4. Rapid turnaround capability.
5. No possibility of damaging gage during test.
6. Preferable to avoid explosives, propellant, or combustible gases.

Frequency response of the measurement system affects to some extent calibrator design. To analyze these effects the measurement system was modeled by a low-pass RC filter, and response to a Brode pressure profile (Reference 2) was directly computed. Details of these calculations will be found in Appendix A.

Air blast data on field tests are usually recorded on oscilloscopes or tape decks. With modern wideband oscilloscopes there is negligible error in recording peak pressure or impulse provided the gage, transmission line, and scope have a bandwidth of 300 kHz or more. This bandwidth is easily surpassed by most oscilloscopes, and approximately equaled by typical high pressure quartz piezoelectric gages. The transmission line is assumed to have negligible attenuation at this frequency. By direct calculation (Appendix A) a system bandwidth of 300 kHz (-3 dB point) results in a peak overpressure measurement error of 1.2% with a 10,000 psi

shock at 1 kiloton yield. This error is less than the standard 3% error for oscilloscopes. The error is even less at longer pulse durations associated with lower overpressures or larger yields.

The situation with a tape deck is quite different. Typical deck bandwidths are 20 kHz, and are the limiting factor in system response when quartz gages are used. Assuming a -3 dB point of 20 kHz, the same 10,000 psi shock from a 1 kT source will have a measured peak overpressure of 9016 psi, or a 9.8% error. However, as is noted in Appendix A, impulse measurements are unaffected by the frequency roll-off of a low-pass filter, and accurate impulse data may be obtained even when peaks are severely degraded. The actual frequency response characteristics of gage plus recording system may be more complex than an RC low-pass filter, but it is probable that impulse measurements will be insensitive to bandwidth.

If peak overpressure and early pressure-time history are to be measured accurately, it is important to maintain a sharp leading edge on the calibration pulse to simulate more closely conditions in a field test. If only impulse measurements are to be recorded, the acceptable recording bandwidth is much lower, and the corresponding pulse rise-time may be much slower. For a general purpose calibrator, the more conservative approach is to require a sharp leading edge in the calibrator pressure pulse.

Required risetime of the calibrator pulse may be estimated from the response of a low-pass filter to a step function (Appendix A). With a -3 dB frequency of 20 kHz, the 10 - 90% risetime at the output is 24μ sec; if the system bandwidth is 300 kHz, the risetime drops to 1.2μ sec. To be useful, therefore, the calibrator risetime must be on the order of 1μ sec or less, which implies a shock wave pressure pulse in the calibrator.

Pulse duration is an important design consideration, particularly when a shock wave is used to generate the pressure pulse, as it directly affects the size of the calibrator. The critical element is the settling time of the gage being measured. Acoustic or mechanical oscillations in a gage cause ringing, and most experimenters have had the unfortunate experience of seeing blast wave records partially or completely obscured by ringing. Typical time scales to damp out ringing can be as short as a few microseconds for well-designed quartz piezoelectric gages, or as long as 2 milliseconds for low pressure gages. The important point with ringing is that high pressure blast wave measurements should use gages which settle reasonably quickly, or a significant fraction of the profile will be lost.

The allowable time scale for settling can be derived from Figure 1, which shows 1,000 and 10,000 psi blast waves from 20 ton and 1 kiloton charges. It is reasonable to

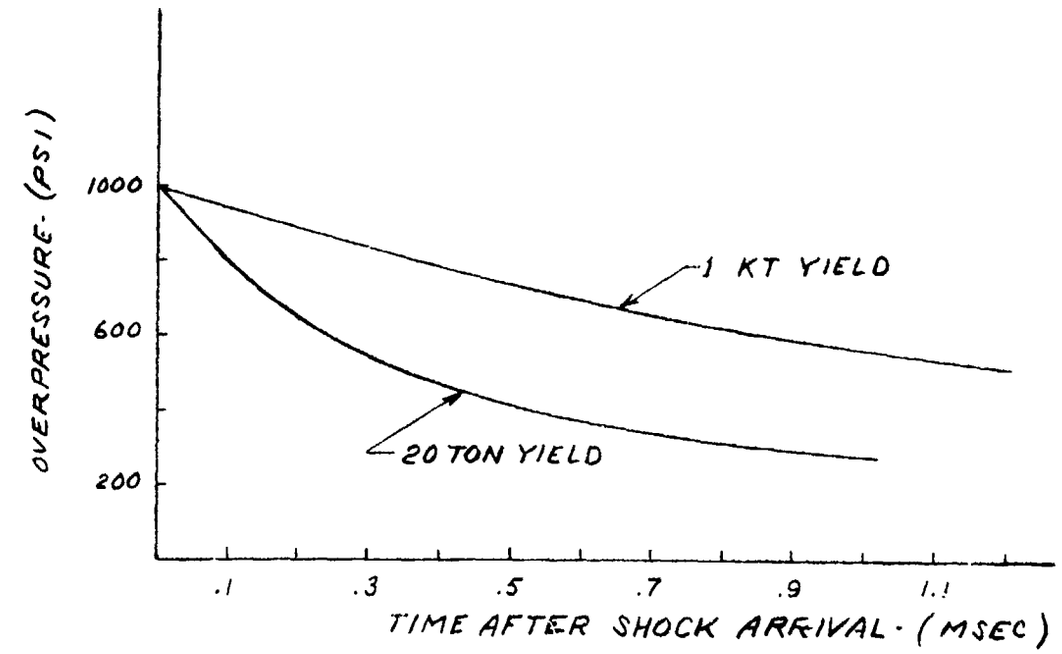

(a) 1,000 PSI BLAST WAVE PROFILE

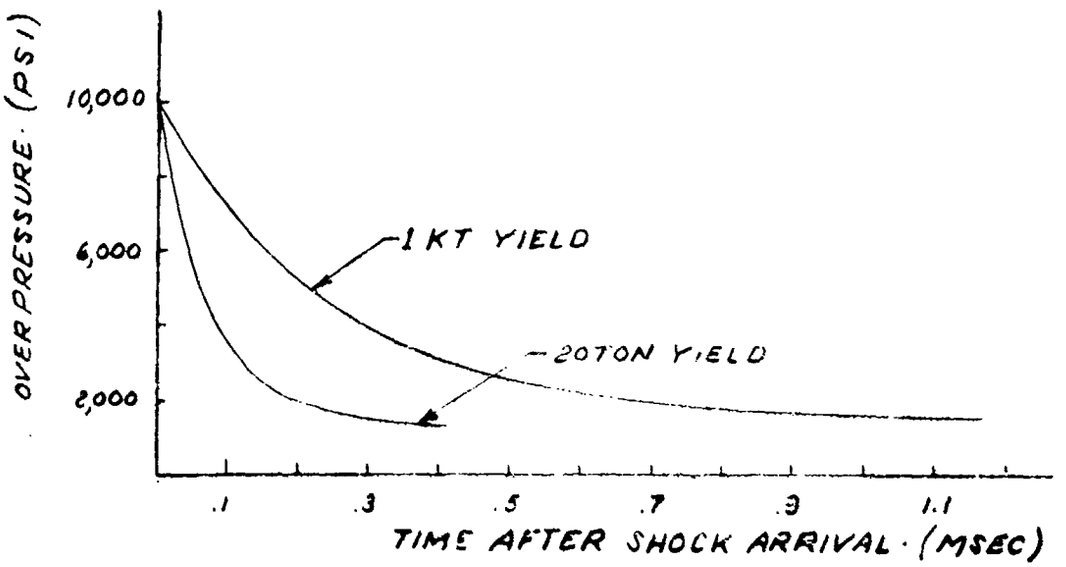

(b) 10,000 PSI BLAST WAVE PROFILE

Figure 1. Blast wave profile for 1 KT and 20 ton yields.

demand that a gage should settle within the time the pressure pulse drops to 90% of the incident shock overpressure. At 10,000 psi the times are 10μ sec and 30μ sec for the 20 ton and 1 kiloton blasts; at 1000 psi the times increase to 50 μ sec and 190μ sec. Gages which settle within these times can use a fairly brief calibration pulse, perhaps 500μ sec duration. A calibrator designed for a 500μ sec pulse obviously will be useless with a gage having a 2 millisecond settling time. Design modifications to convert a short duration high-pressure calibrator into a long duration low-pressure calibrator will be discussed later.

3. DESIGN STUDY FOR HIGH PRESSURE CALIBRATOR

A wide range of techniques for pressure testing an air blast gage were considered during this program. Performance data on all system concepts are presented, even though some methods do not meet the criteria for a field portable system. In this way the data is available for reevaluation when the need arises for different performance or system requirements.

The pressurization techniques have been split into three general classes: standard shock tubes, inverted shock tubes, and shockless systems. The standard shock tube, consisting of a high pressure driver and a low pressure driven section, is well known and needs no further introduction. The inverted shock tube is a novel configuration which was developed for this application; the high pressure shock tube driver is expanded and shortened to form a reservoir, and the driven tube is folded back into the high pressure section. The inverted shock tube is more compact than the usual shock tube, although the principles of operation remain the same. A detailed discussion of the inverted design, with figures, is given later.

The final category of systems are called shock free because they do not have a well-formed, planar shock wave at the gage face. A typical system would be a large reservoir separated by a diaphragm from a gage housed in a small recess.

The diaphragm ruptures to pressurize the gage, but the run-in to the face is too short for a strong shock to form. The pressurization is best described as an acoustic mass flow into the recess. Note that weak, nonplanar shocks may be present here, so the term shock free is only relatively correct.

Performance data on each class of systems are presented in the following subsections. It is not possible to include all details of the performance calculations, so the emphasis here is on the assumptions for the calculations, the limitations on performance, and some representative test times.

3.1 Standard Shock Tube Systems

The design and operation of conventional shock tube systems is a well-developed field, so a detailed description of shock tube principles will not be given here. The gas-dynamic wave system in a constant area shock tube is described in Reference 3. Reference 4 is a general reference work on shock tubes. It contains basic theory plus design charts for a wide variety of shock tube systems.

Table 1 presents performance data for the shock tube systems analyzed during this study. The first four columns show the driver and driven tube condition, area ratio between driver and driven tube, and the maximum reflected pressure with a 10,000 psi limitation in the driver and a 150 psi limit in the driven tube. These upper limits were chosen

Table 1. Standard shock tube performance data.

Driver	Driven Tube	Area Ratio	Max. Reflected Pressure - 10,000 psi Reservoir (psi)	Reflected Shock Pressure (psi)	Incident Shock Pressure (psi)	Shock Temperature Reflected (K)	Shock Temperature Incident (K)	Reflected Test Time (msec)	Size on Test Time (msec) Const P	Size on Test Time (msec) Const T
Compressed air	1 atm air	1	750	---	---					
Compressed air	10 atm air	1	9,100	1,000	410	530	400	4.2	5.0	3.*
Compressed air	1 atm air	4	990	990	160	1,500	880	.85	1.3	.50
Compressed air	10 atm air	4	4,100	4,100	1,000	940	600	1.5	3.4	1.0
Compressed He	1 atm air	1	9,100	1,000	184	1,500	880	.85	1.3	.59
Compressed He	10 atm air	1	10,000	1,000 10,000	410 1,850	530 1,500	400 880	.38 .85	.65 1.3	.65 .59
Compressed He	1 atm air	4	4,900	4,900	590	3,500	2,000	.40	.90	.25
Compressed He	10 atm air	4	15,500	15,600	2,580	2,000	1,100	.70	1.5	.47
Combustion H_2-O_2-74% He	1 atm air	1	10,000	1,000 10,000	184 1,120	1,500 5,500	880 3,100	.00 .18	.07 .62	.07 .11
Propellant (1 Megajoules/pound)	1 atm air	1	10,000	1,000 10,000	184 1,120	1,500 5,500	880 3,100	.47 .17	.64 .77	.55 .10
Electric Arc	1 atm air			1,000	Capacitor bank too large to be portable. See text for details.					

NOTES
1. Test times are ideal.
2. Reflected test time is duration of constant pressure from the first reflection.
3. Drivers are 100 cm long, driven tubes are 900 cm long.

to keep the system weight down for portability.

The remainder of the table shows performance at a specific design point. Shock pressure and temperature behind the incident and reflected waves are indicated, along with test times. The test times were calculated for a 100 cm long driver and a 300 cm long driven tube. The test station for the incident wave is 200 cm downstream from the diaphragm. The test times in the table are uncorrected for non-ideal effects.

The performance of the constant area, compressed gas tubes is described in detail in Reference 4. Design charts from Reference 4 give P_{41} vs. P_{21}, or the ratio of reservoir to ambient driven pressure versus the pressure ratio across the incident shock. Real air tables (Reference 5) or reflected shock tables from Reference 4 were used to compute reflected shock pressure.

The performance of compressed gas tubes with an area contraction was calculated from first principles. The wave system in the tube has an unsteady expansion propagating back into the driver followed by a steady expansion to a Mach number of 1 at the throat, the entrance to the driven tube. In the driven section there is a further unsteady wave system to equilibrate to a point on a shock Hugoniot. Calculations assumed a gas with constant isentropic exponent.

The area contraction of 4 was chosen because the relative sizes of driver and driven sections are still

reasonable, and because a much larger area contraction does not significantly improve performance. Additional calculations with an area contraction of 20 increased the maximum reflected pressures by at most 20%.

Design of a combustion driven shock tube used the design charts in Reference 4. The driver mixture was an oxygen-hydrogen-helium combination with 79% helium. This particular mixture was chosen for intermediate performance among all the combustible gas combinations listed.

The 10,000 psi reflected pressure point in Table 1 can be designed directly from charts for combustion drivers in Reference 4. The low pressure, 1000 psi point cannot be designed from the charts and has been calculated from the ideal shock tube equation relating P_{41} and P_{21} derived in Reference 3. The value of γ was 1.4.

The performance of a propellant driven shock tube was also calculated with the ideal shock tube equation. The propellant energy was 2 Megajoules per pound, which is a typical value for most propellants or explosives. The isentropic exponent of the combusted and expanded gaseous products was taken as 1.4. Any errors resulting from variations in the exponent should be small. The amount of propellant required for the high performance state is small -- less than 1 pound for a 10 cm inner diameter by 100 cm long driver.

The final system considered was an electric arc discharge shock tube. No performance data is given for this driver in Table 1 because the capacitor bank required to achieve even a 1000 psi reflected shock is quite large and unportable. For example, with 20 atmospheres of helium in the driver, as is suggested in Reference 6, and assuming the energy transfer is 20% efficient (Reference 4), a 120 kilojoule capacitor bank is required for a 1000 psi reflected shock. This power supply requirement is probably optomistic because it is difficult to achieve a 20% efficiency in the arc discharge. The large size of the power supply combined with the existance of alternate methods to achieve the same performance made this approach impractical and further performance calculations were not performed.

Table 1 shows that none of the air/air systems can achieve a 10,000 psi reflected state with the constraints of less than 10,000 psi in the reservoir and 10 atmospheres in the driven tube. A helium/air system can achieve the required performance, with 10 atmospheres in the driven section. The tradeoff between helium versus air in the driver is that test times are sharply reduced along with increased performance and complexity for a helium system. If the performance criteria were reduced to a peak reflected pressure of 3000 psi, then an air/air system would be attractive.

The combustion and propellant driven tubes can easily achieve the high pressure states, but test times are extremely short. In addition, the detonable gases or propellant are undesirable in the field from a safety viewpoint.

Finally, the shock tube systems are rather long -- 12 feet -- to achieve the test times in Table 1. Although the tube can be scaled up or down, with corresponding changes in test times, the general configuration of a conventional shock tube is not optimal for a portable system. An alternate shock tube configuration, more appropriate for a field portable system, is discussed below.

3.2 Inverted Shock Tubes

The inverted shock tube consists of a large, high pressure reservoir and a small diameter, low pressure driven tube, separated by a diaphragm. Figure 2 shows this design, which operates as a shock tube with a large area contraction between the driver and driven section. The driven tube has been folded back into the reservoir for compactness, hence the term inverted shock tube. The pressure gage is placed at the end of the driven tube, where it responds to a normally reflected shock wave.

Design calculations for the inverted tube must be performed from first principles. The wave system is similar to the gasdynamics of a standard shock tube with an area

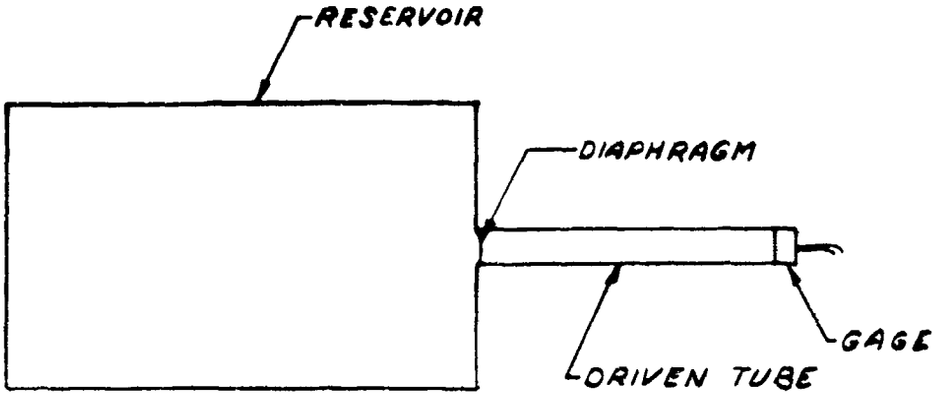

(a) SHOCK TUBE WITH LARGE AREA CONTRACTION

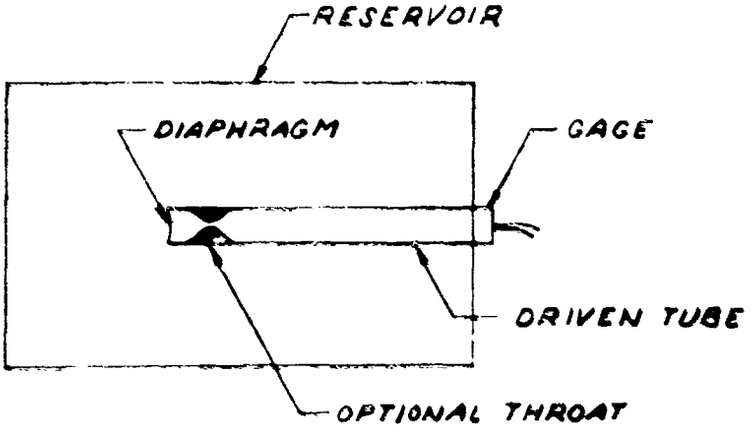

(b) INVERTED SHOCK TUBE

Figure 2. Conventional and inverted shock tubes.

contraction. For simplicity, the area ratio between reservoir and driven tube is assumed infinite, so the unsteady expansion propagating back into the reservoir has zero strength and is ignored. The gasdynamic process then becomes a steady expansion to Mach number 1 at the driven tube entrance followed by an unsteady expansion to equilibrate to a point on the shock Hugoniot. Figure 3a shows this wave system.

The gasdynamic process can be modified by adjusting one, or possibly two free parameters in the inverted system. The first parameter is the ratio of reservoir to driven pressure, which is always available. A second parameter can be created by placing a throat in the driven tube, so the area ratio of the throat to driven tube is variable. If the throat is included the steady wave system expands the gas to a Mach number greater than 1 before the unsteady expansion begins.

Adjusting the gasdynamic process with these two parameters can produce a system with longer test times or a more convenient mode of operation. Typical conditions which can be satisfied are:

1. Eliminate the unsteady rarefaction at the entrance to the driven tube;
2. Match states at the contact surface so the reflected shock does not interact with the interface; and

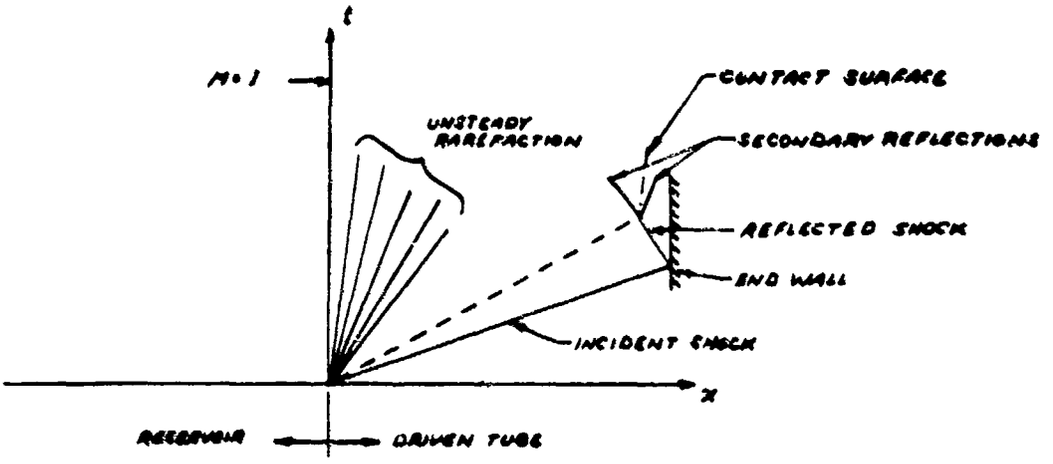

(a) TYPICAL WAVE SYSTEM

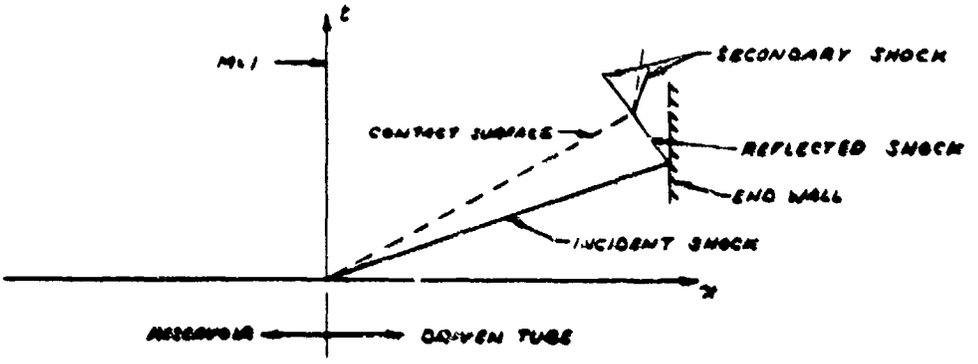

(b) SYSTEM MATCHED TO ELIMINATE UNSTEADY RAREFACTION

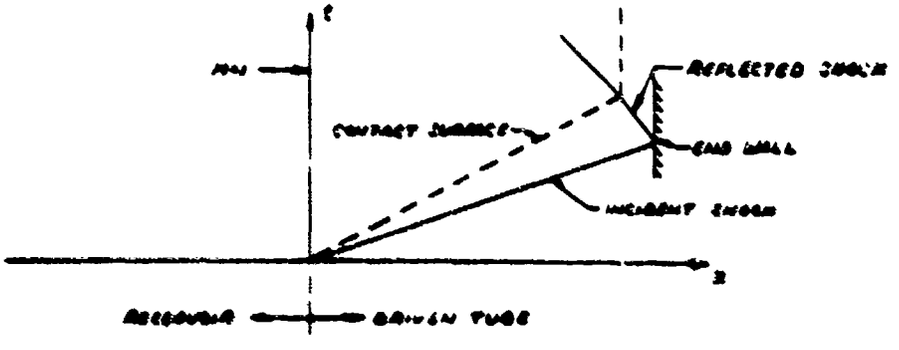

(c) UNSTEADY RAREFACTION ELIMINATED AND SYSTEM MATCHED AT THE CONTACT SURFACE

Figure 3. Typical wave system in the inverted shock tube.

3. Specify that the initial reflected pressure equals the reservoir pressure.

The first two conditions will tend to increase test time while the last condition will simplify operation of the inverted shock tube. Figures 3b and 3c show the effect on the wave system of condition 1 and conditions 1 and 2 together.

If the second condition is not satisfied, the wave system reflected from the contact surface will arrive back at the gage face and significantly alter the magnitude of the reflected pressure from the incident shock. Further reflections will occur as the wave system travels between the contact surface and gage face, giving the leading edge of the pressure pulse a stair-step structure.

Many design options were investigated for the inverted tube. These are listed in Table 2, including the reservoir and driven tube gas and the special conditions imposed on the operational mode. Note that it is impossible to design an air/air system which is matched at the contact surface, if both reservoir and driven tube gases are at the same temperature.

Five inverted systems were selected for more detailed design calculations. The results of these calculations are found in Table 3. The entries in this table include the reservoir and driven tube gases, the operating mode, the

Table 2. Design options investigated with the inverted shock tube.

Reservoir/Driven Gas	Operating Mode
Air/Air	Unsteady wave system eliminated
Helium/Air	Unsteady wave system eliminated
Helium/Helium	Unsteady wave system eliminated
Air/Air	Reservoir pressure = reflected pressure
Helium/Air	Reservoir pressure = reflected pressure
Air/Air	Reservoir pressure = reflected pressure and unsteady wave system eliminated
Helium/Air	Matched at contact surface
Helium/Air	Matched at contact surface and unsteady wave system eliminated
Air/Air	Matched at contact surface - IMPOSSIBLE

Table 3. Detailed design data on five inverted shock tube operating modes.

Case No.	Reservoir/ Driven Gas	Operating Mode	A_1/A_4	P_4/P_1	P_5/P_4	Initial Reflected Pressure (psi)	Duration (μsec)	Second Reflection (psi)	Duration (μsec)	Final Pressure (psi)
1	Air/Air	No unsteady wave	1	5.98	1.42	1,000	710	1,250	500	1,400
2	Helium/Air	No unsteady wave	1	26.6	2.68	1,000	160	720	140	
3	Air/Air	$P_4 = P_5$	1	15.6	1	1,000	460	1,580	260	1,800
4	Air/Air	No unsteady wave, $P_4 = P_5$	1.12	13.7	1	1,000	500	1,510	290	
5	Helium/Air	No unsteady wave, matched at contact surface	1.07	59.6	1.58	1,000	1,400	---	---	

NOTES: 1. Driven tube 24" long.

2. Infinite area ratio between reservoir and driven tube.

3. Test times ideal.

area ratio of driven tube to throat, and the ratio of reservoir pressure (P_4) to driven tube pressure (P_1). These two ratios remain constant to maintain the desired operating mode, independent of the magnitude of the reflected pressure. The pressure ratio of the initial reflected pressure (P_5) to the reservoir pressure is also given.

The remainder of the table shows initial pulse durations for a driven tube 24-inches long with an initial reflected pressure of 1000 psi. The second pressure step generated by reflection off the contact surface and its duration are also listed in Table 3. The test times in the table are ideal, so contact surface spreading and other non-ideal effects may reduce the times by as much as 50%.

For the air/air systems, the second pressure jump can increase the initial gage pressure by more than 50%. With the helium/air system which is mismatched at the contact surface, the gage pressure decreases because a rarefaction, rather than a shock, reflects off the contact surface.

If a system is unmatched at the contact surface, the sequence of pressure jumps decreases in amplitude to form a broad, approximately constant pressure pulse at the gage face. The magnitude of the constant pulse, which will not equal the initial reflected pressure, is shown in the last column of Table 3 for two cases. The value for system #3 comes from hydrodynamic code calculations, while the final

pressure for system #1 was calculated by hand. A pressure-time history and wave diagram for the first system are presented in Figures 4 and 5. The dashed line in Figure 4 represents ideal behavior, and the pressure plateau will not be absolutely constant. Following the constant pulse, the pressure at the end wall oscillates or rings in a manner similar to an organ pipe. Viscous effects will eventually damp out the ringing.

The form of the pressure pulse creates two options for calibrating pressure gages. Systems with a frequency response high enough to follow the individual stair-steps can use the steps as multiple calibration points. Low frequency response systems will smooth out the structure of the pulse's leading edge so the broad, constant pressure portion of the pulse can be used to calibrate a gage. Which mode of calibration will be most effective will depend on the chosen gage and recording system and is difficult to specify in advance.

System #5, which is matched with no unsteady wave system or reflections off the contact surface, produces a very long test time (1.4 milliseconds) at 1000 psi. This is almost a factor of two greater than the best, unmatched system. Unfortunately this matching cannot be achieved without the additional complexity of a dual gas system, or heating the reservoir gas.

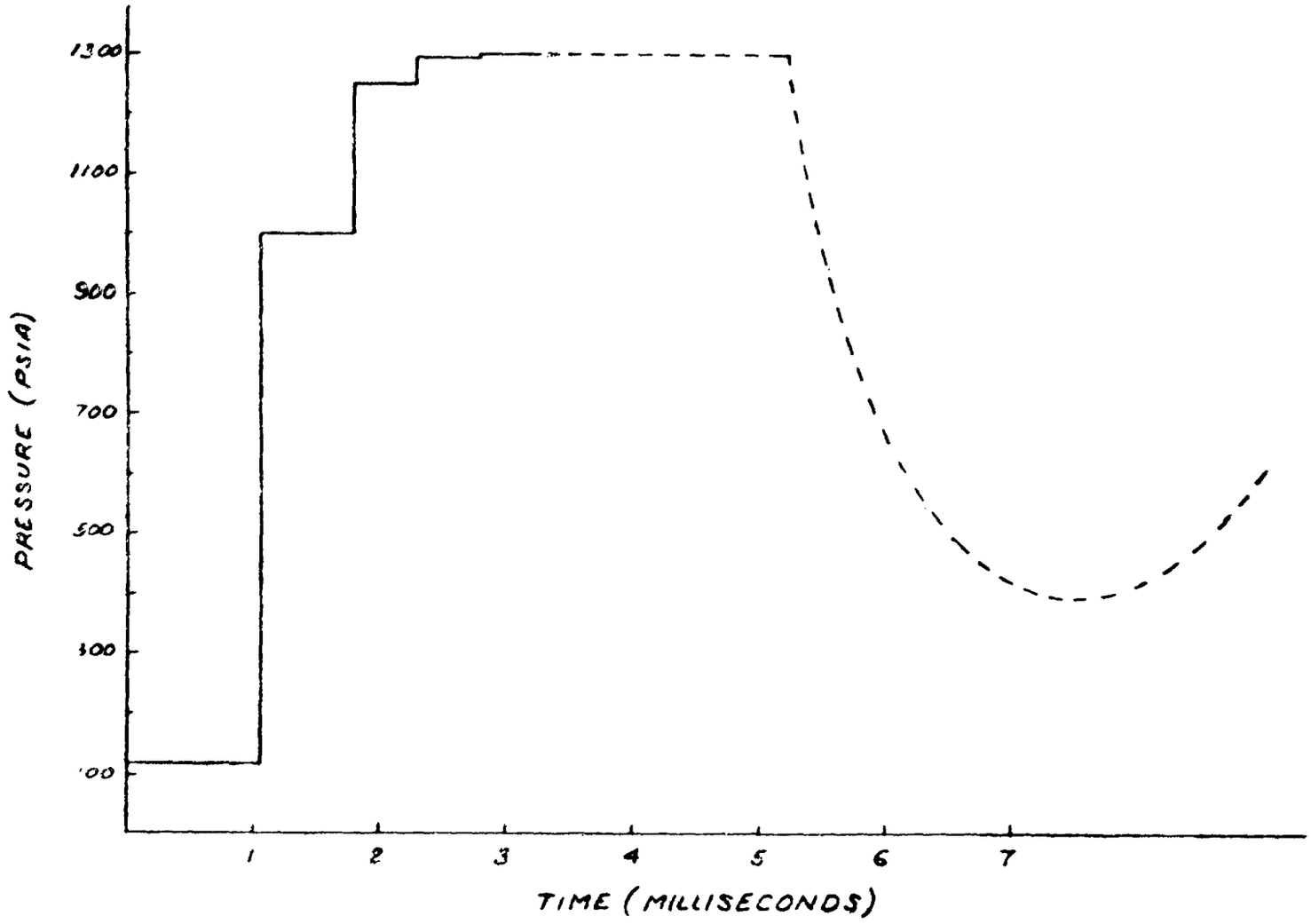

Figure 4. Pressure-time history at the gage face for an inverted shock tube operating in the preferred mode.

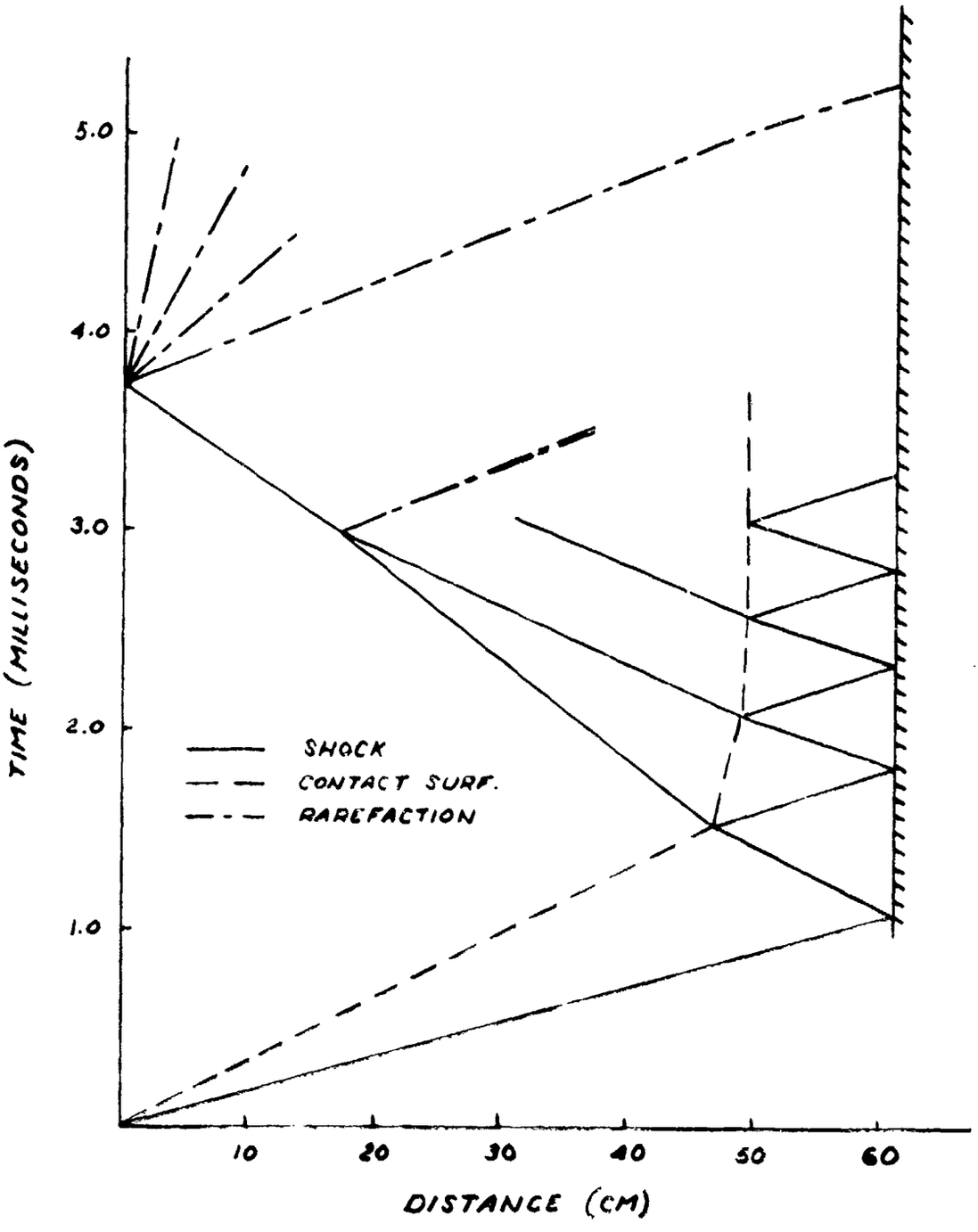

Figure 5. Wave diagram for an inverted shock tube operating in the preferred mode.

Among the five systems listed in Table 3, the first air/air configuration seems most appropriate for field use. Designs with a helium filled reservoir require carrying additional gas bottles at increased cost. The two air/air designs which match reflected and reservoir pressure will be heavier than the first system, because the chamber must be designed for the full reflected pressure. With system #1, the chamber can be designed to 70% of the reflected pressure. Further design details will be given for the first system in a later section.

3.3 Shockless Systems

The final category of calibration systems do not have a well-formed, planar shock wave incident upon the face of a pressure gage. Two typical designs which fall within this classification will be discussed here. Both designs are distinguished by the difficulty of calculating the exact shape of the pressure pulse at the gage face and only rise-time estimates will be made in this section.

The first shockless system is a reservoir with a small recess. A diaphragm separates the recess from the main chamber and a pressure gage is located at the bottom of the recess. The calibration pulse is produced when the diaphragm breaks and gas flows into the recess. The depth of the recess is great enough for the diaphragm to petal open

smoothly without striking the gage, but too short for a strong shock to coalesce. A typical depth is two to four recess diameters.

The risetime of the pressure pulse at the gage depends on the opening of the diaphragm and on the subsequent flow of gas into the recess. The opening time can be estimated from a strengthless analysis, calculating the time required for the diaphragm material to move a specified distance with a given pressure differential. For example, a 1 cm diameter recess with a 1000 psi differential needs an aluminum diaphragm .022-cm thick or a steel diaphragm .004-cm thick (Reference 4). If the diaphragm moves 1 cm to open, then the opening times are 40μ sec with aluminum and 30μ sec with steel.

The flow of gas into the recess can be estimated from a steady state analysis. Assuming sonic velocity at the entrance to the recess, the time to fill the recess to the same density as the reservoir gas is given by:

$$\Delta t = \left(\frac{\gamma+1}{2}\right)^{\frac{\gamma+1}{2(\gamma-1)}} \cdot \frac{\ell}{a_1}$$

The quantity γ is the isentropic exponent, ℓ the depth of the recess, and a_1 the reservoir sound speed. If the recess is 2 cm deep, an air or helium filled reservoir takes

100 μ sec or 35 μ sec, respectively, to fill the recess.

Combining both estimates, the probable pulse risetime is on the order of 100 - 200 μ sec for a 1-cm diameter by 2-cm deep recess. Following the initial rise and peak there will be ringing as the recess equilibrates to the reservoir pressure. If several acoustic transits are required for the equilibration, a total of several hundred microseconds will elapse before the recess pressure equals the reservoir pressure. Although the equilibration time is rather long, this calibration system might be adequate for gages measuring impulse, where risetime requirements are not especially important.

The second technique for pressure testing a gage is based an a fast acting piston. Again there is a high pressure reservoir with a gage flush mounted on the inside wall. A small, fast acting piston seals the gage at ambient pressure. The pressure forces on the piston are balanced such that a slight break in the gas seal will shoot the piston backwards, away from the wall, and allow the high pressure gas to load the gage. This type of piston can be built and has been successfully used in light gas guns to rapidly pressurize a projectile for launch.

Calculation of the pressure pulse at the gage is extremely difficult. The time scale can be estimated from the motion of the piston. A light, 8 oz piston with 1000

pounds of force requires 1.5 milliseconds to move 1 inch. This time scale is much longer than the equilibration time for the recessed gage with a diaphragm, and almost comparable to the BRL low pressure calibrator. Both these facts make the fast acting piston unattractive for pressure gage calibration.

4. PRELIMINARY ENGINEERING DESIGN OF INVERTED SHOCK TUBE

4.1 Selection Rationale

Many of the techniques presented above provide credible and effective means for calibrating pressure gages with high overpressure pulses, but the specified design criteria strongly favor the inverted shock tube concept.

The standard shock tube is a long, slender cylinder far less portable than the short, compact, inverted shock tube. Another drawback to the standard shock tube is the difficulty of achieving the required performance within a reasonable driven tube pressure limitation (10 atm); the inverted shock tube has a driven tube within the high pressure driver chamber, so it can operate at much higher initial pressures without a weight penalty.

The shockless system consisting of a reservoir with a recessed gage, activated by a diaphragm, is unsuitable for high pressure calibrations because it produces a slowly rising (100 μ sec) pressure pulse which rings for several hundred microseconds. It is desireable to have a sharp leading edge on the pressure pulse to simulate more closely actual blast wave loading. On the other hand the shockless system may be ideal for low frequency, low pressure gages, which in some cases take nearly 2 milliseconds to settle.

The inverted shock tube combines the advantages of compactness and reasonable weight with a sharp leading edge

on the pressure pulse, and closely satisfies the design criteria for a field portable calibrator. Among the five operating modes of the inverted shock tube listed in Table 3 the first (#1) is the recommended system for portable applications. The two modes requiring a helium-filled reservoir are less practical for field applications than an air-filled reservoir. Of the air/air concepts the first is more practical because a 10,000 psi pressure pulse is achieved with only 7,000 psi in the reservoir. The other two air/air concepts (3 and 4) require 10,000 psi in the reservoir for a 10,000 psi reflected pressure pulse in the driven tube, implying a heavier and more costly structure.

The pulse shape of the preferred inverted shock tube concept consists of a sharp-rising initial pulse followed by stair-step increases to a broad, approximately constant pressure plateau (Figure 4). The stair steps result from reflections between the end wall and the contact surface. Ideal durations of the first two steps are 710 μ sec and 500 μ sec, assuming a 24-inch long driven tube. Duration of the broad pressure plateau is estimated to be 2 milliseconds from a calculation of the ideal wave system (Figure 5). Non-ideal effects, such as contact surface mixing and boundary layers, may reduce these ideal times by as much as 50%, and will smear out the stair step pulses corresponding to reflections from the contact surface.

High-pressure, fast-response gages may be calibrated

by using the sharp-rising initial pulse; subsequent levels in the stair-step pulse may serve as additional calibration points in the same test. Lower frequency gages unable to follow the individual steps in the pressure pulse may be calibrated at the broad pressure plateau.

An added advantage of the inverted shock tube concept is that it is readily converted to a shockless system ideal for calibrating low-pressure, low-frequency gages. The conversion is accomplished by having a driven tube which can be shortened and capped with a diaphragm to create a recess.

The inverted shock tube concept, from several points of view, is clearly superior to alternate calibration systems, and is the recommended system for further design and development. It is compact, portable, and safe to operate; it is based on classic shock-tube design with clearly understood, predictable, and reproducible principles of operation; and it generates a pressure pulse capable of calibrating a broad spectrum of pressure gages, from high-pressure, high-frequency gages to low-pressure, low-frequency gages.

4.2 Engineering Design and Cost Analysis

A preliminary engineering design study and component cost analysis for the recommended calibrator concept was carried out jointly with Beam Engineering, Inc. The design satisfies all performance and operational criteria of

Section 2, and is capable of generating a sharp-rising pressure pulse up to 10,000 psi (with peak pressure, after a stair-step rise, to 13,000 psi).

Calibrator system layout is shown in Figure 6. It consists of a calibrator, air bottles, battery powered pressure intensifier, cable hoist, and control unit, all mounted on a pallet to fit into a pickup truck.

In field use the calibrator may be used in the truck for gages with sufficient cable slack, or it may be lifted from the truck and attached to an in situ gage. The intensifier equipment was sized to pressurize the chamber to the required 7,000 psi (for a 10,000 psi pulse) in 7 minutes, and the calibrator is designed for quick turnaround in conducting tests. It is estimated that tests could be conducted every 24 minutes at maximum conditions, or 25 tests in a 10-hour day.

The calibrator, shown in Figure 7, is designed to the ASME boiler and pressure code, and to the California State Code. It is completely safe for nearby personnel during operation. It includes a solenoid actuated diaphragm punch, so the timing of the calibration pulse can be electronically controlled. The calibrator lid has a quick-release buttress thead requiring only a partial turn to open, allowing the diaphragm to be replaced repeatedly without disconnecting the calibrator from the gage. The required ratio of chamber

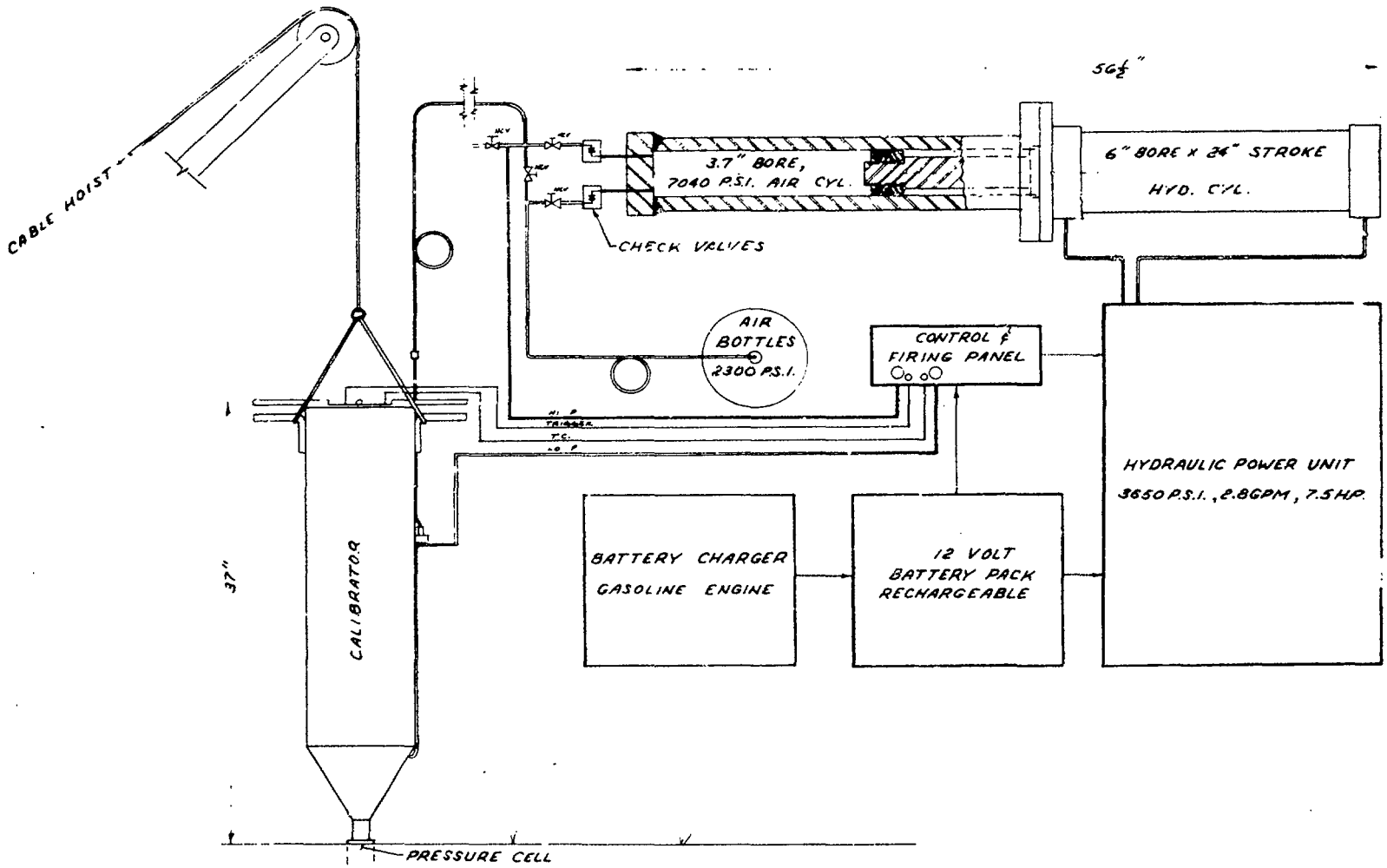

Figure 6. Pressure gage calibrator system layout.

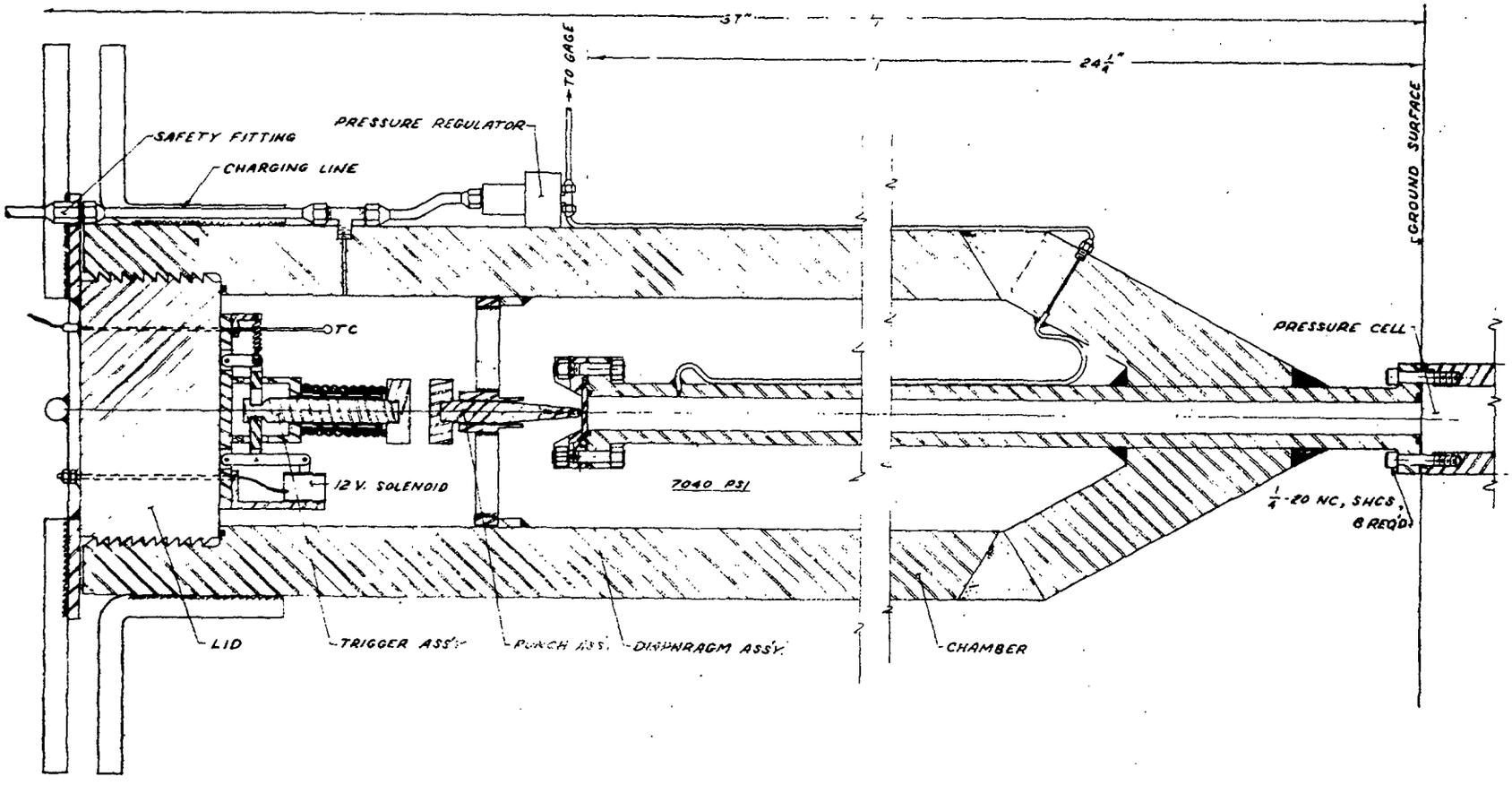

Figure 7. Pressure gage calibrator.

pressure to driven tube pressure is maintained by a differential pressure regulator, and a single pressure reading is sufficient to establish the operating point of the calibrator.

For chamber pressures up to 2100 psi standard air bottles are sufficient. This value corresponds to an initial sharp-rising pulse amplitude of 3000 psi and a peak amplitude of 3900 psi. Higher pressures require the use of the battery-powered hydraulic pressure intensifier consisting of a 3.7-inch bore, 24-inch stroke air cylinder, a hydraulic power unit, and a battery pack with gasoline engine recharger. The maximum design chamber pressure of 7040 psi is achieved with 3 cylinder strokes.

An engineering cost estimate of fabrication and assembly of the 10,000 psi calibrator system is shown in Table 4. It does not include one-time engineering and development costs, and it does not include costs associated with management, bid evaluation, and contract monitoring. It includes all direct costs associated with component purchase and fabrication, together with an estimate of general contractors overhead and profit, and represents an engineering estimate of the total cost of fabrication and assembly. No provision has been made for cost escalation, but an overall contingency allowance of 15% has been applied in recognition of the unique nature of the system. Pressure components are assumed to be fabricated in shops certified by ASME to afix the code symbol

Table 4. Cost analysis of 10,000 calibrator system.

Calibrator Components		
Chamber	$ 4,690	
Lid	1,520	
Punch Assembly	800	
Trigger Assembly	960	
Pressure regulator	1,600	
Fittings, tubing	200	
Thermocouple	200	
Diaphragms (1000)	1,000	
Subtotal		$10,970
Pressure Intensifier Components		
Air Cylinder	$ 3,240	
Piston	180	
Hydraulic Cylinder & Pump System	2,600	
Battery Pack	400	
Battery Charger Engine	750	
Subtotal		$ 7,170
Operational Components		
Firing Panel, meters, wiring	$ 80	
Crane Hoist, monorail, 1/2 ton	1,000	
Skid mount pallet	500	
Pressure tubing, valves, fitting	250	
Subtotal		$ 1,830
Total Component Costs		$19,970
Direct Labor		
Assembly, Calibration, and Test		3,200
Subtotal		$23,170
Contingencies @ 15%		3,480
Contractors Overhead & Profit @ 25%		5,800
Engineering Cost Estimate		$32,450

for an unfired pressure vessel, and to undergo the required inspection and documentation.

A major portion of the calibrator cost is related to pressure intensifying equipment required to develop 7000 psi chamber pressure, and considerable savings may be accomplished by restricting performance to bottle pressure levels. At 2100 psi chamber pressure the initial pressure pulse is 3000 psi. An engineering cost estimate of the 3000 psi calibrator is shown in Table 5. Considerable savings are evident in the calibrator fabrication because of reduced requirements, and the pressure intensifier costs are eliminated.

In field tests a calibrated pressure gage (not shown in Figure 7) would be installed in the driven tube side wall for dynamic verification of the calibrator pulse amplitude. This pressure gage and associated recording instrumentation, both standard equipment, is not included in the calibrator cost estimates.

Table 5. Cost analysis of 3,000 psi calibrator.

Calibrator Components	$ 5,550
Operational Components	1,830
Direct Labor	1,000
Subtotal	$ 8,330
Contingencies @ 15%	1,250
Contractor Overhead and Profit @ 25%	2,090
Engineering Estimate	$11,670

5. CONCLUSIONS AND RECOMMENDATIONS

An inverted shock tube is the preferred concept for a field-portable pressure gage calibrator capable of operating in the 100 - 10,000 psi range. The recommended system meets all the performance and operational criteria specified by DNA and the user community.

A preliminary engineering design study indicated a fabrication cost of approximately $32,450 for a 10,000 psi calibrator system. Much of this cost is related to a pressure intensifier to produce the required 7000 psi chamber pressure. A lower performance system, able to achieve a 3,000 psi pressure pulse with standard bottle pressure in the chamber, would cost approximately $11,670. These costs relate only to fabrication of the unit; they do not include one-time engineering design costs or development tests.

It is recommended that development tests be conducted with an inexpensive laboratory mockup of the inverted shock tube concept operating at bottle pressure. In this way calibrator pressure pulses up to 3,000 psi may be obtained, and details of the design can be modified to optimize calibrator pulse shape and to streamline operational procedures.

REFERENCES

1. Baker, W. E., "Explosions in Air", University of Texas Press, Austin, 1973, pp. 137-149.

2. Brode, H. L., "Review of Nuclear Weapons Effects", Annual Review of Nuclear Science, Vol. 18, 1968.

3. Liepmann, H. W., and Roshko, A., "Elements of Gasdynamics", Wiley, 1967.

4. Glass, I. I., and Hall, J. G., "Handbook of Supersonic Aerodynamics, Section 19, Shock Tubes", NAVORD Report 1488, (Vol. 6), December 1959.

5. Lewis, C. H., and Burgess, E. G., "Charts of Normal Shock Wave Properties in Imperfect Air", AEDC-TDR-64-43, March, 1964.

6. Dannenberg, R. E., and Silva, A. F., "Arc Driver Operation for Either Efficient Energy Transfer or High-Current Generation", AIAA Journal, 10, No. 12, December 1972, pp. 1563-1564.

7. Dannenberg, R. E., "A Conical Arc Driver for High-Energy Test Facilities", AIAA Journal, Vol. 10, No. 12, December 1972, pp. 1692-1694.

APPENDIX A. RESPONSE OF A LOW PASS RC FILTER TO A BRODE PROFILE

We will assume, as a first order approximation, that a pressure gage, transmission line, and recording equipment can be modeled as a low pass RC filter. The arrangement of components is shown below:

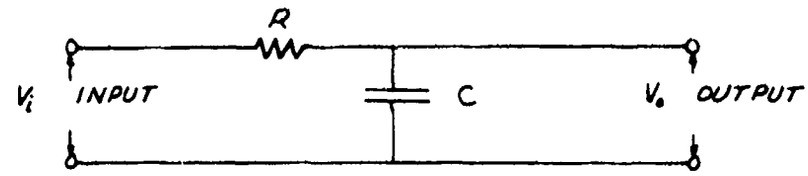

Figure A1. Low pass filter.

The frequency response of the filter can be characterized by $\tau\,(=RC)$, the time constant of the filter, or by f_c, the frequency at which the response is down by 3 dB. Standard definitions from electrical engineering show that τ and f_c are related by:

$$\tau = \frac{1}{2\pi f_c} = \frac{1}{\omega_c}$$

For example, if f_c is 20 kHz, then τ is 8 μ sec.

With a given value of f_c, the response to a Brode profile (Reference 2)

$$V_i = \Delta P_s (1-\bar{t})(Ae^{-\alpha\bar{t}} + Be^{-\beta\bar{t}} + Ce^{-\gamma\bar{t}})$$

where $\bar{t} = t/D$,

may be computed. The quantity ΔP_s is the incident shock overpressure, D the duration of positive phase, and t the time. The parameters A , B , C , α , β , and γ are given as a function of ΔP_s .

The circuit equations for the filter are

$$V_i = iR + \frac{1}{C}\int i\,dt$$

$$V_o = \frac{1}{C}\int i\,dt$$

where V_i and V_o are input and output waveforms, respectively. The equations are linear so it suffices to consider a V_i given by the first term in the profile, solve the equations, and add two additional terms of the same form. Omitting the long algebraic details of finding a solution to the first order equations, the leading term for V_o is given by

$$V_o = \Delta P_s (A\omega_c)\left[\frac{(D\omega_c - \alpha - t\omega_c + \frac{t\alpha}{D} + 1)\,e^{-\alpha t/D} - (D\omega_c - \alpha + 1)\,e^{-t\omega_c}}{(D\omega_c - \alpha)^2}\right]$$

Numerical values for V_i were found for a wide range of f_c using a digital computer. A typical measured profile is shown in Figure A2 for a 20 kHz filter and a 10,000 psi overpressure shock from a 1 KT yield. The Brode parameters for this wave are

$A = .0214$ $\quad \alpha = 4.985$

$B = .1718$ $\quad \beta = 41.33$

$C = .8068$ $\quad \gamma = 617.6$

$D = .1416$

It is evident from Figure A2 that a significant error in the measured peak overpressure can exist. For the above case, it equals 9.8%. The variation of the error with f_c for the same 10,000 psi shock wave is shown in Figure A3.

Another important airblast parameter is the measured impulse, which can be evaluated directly from the differential equation:

$$V_i = iR + V_o$$

so

$$\int_o^t V_i = R \int_o^t i\,dt + \int_o^t V_o\,dt$$

or

$$\int_o^t V_i = \tau V_o + \int_o^t V_o\,dt$$

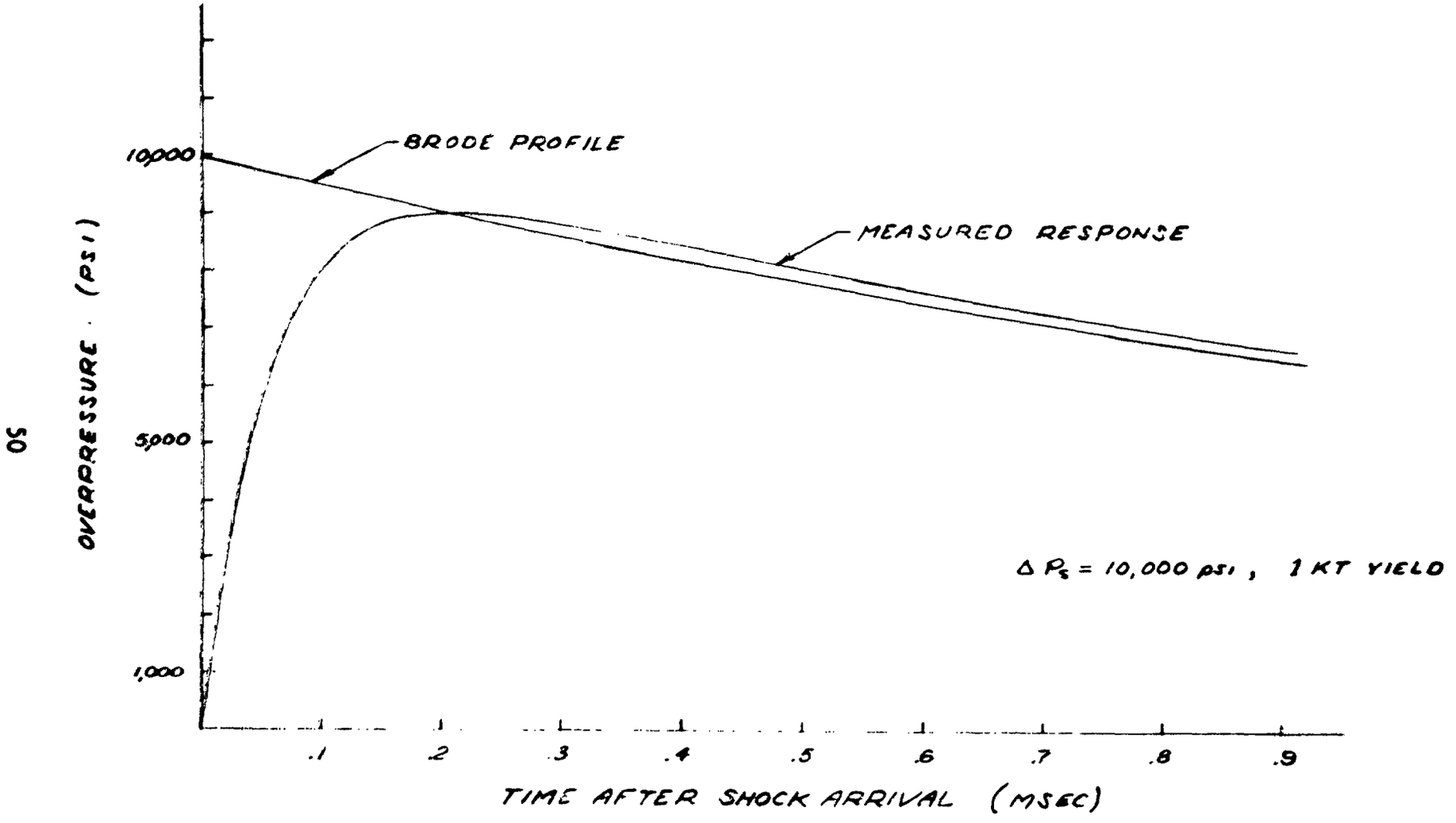

Figure A2. Brode profile and response through a 20 kHz low pass filter.

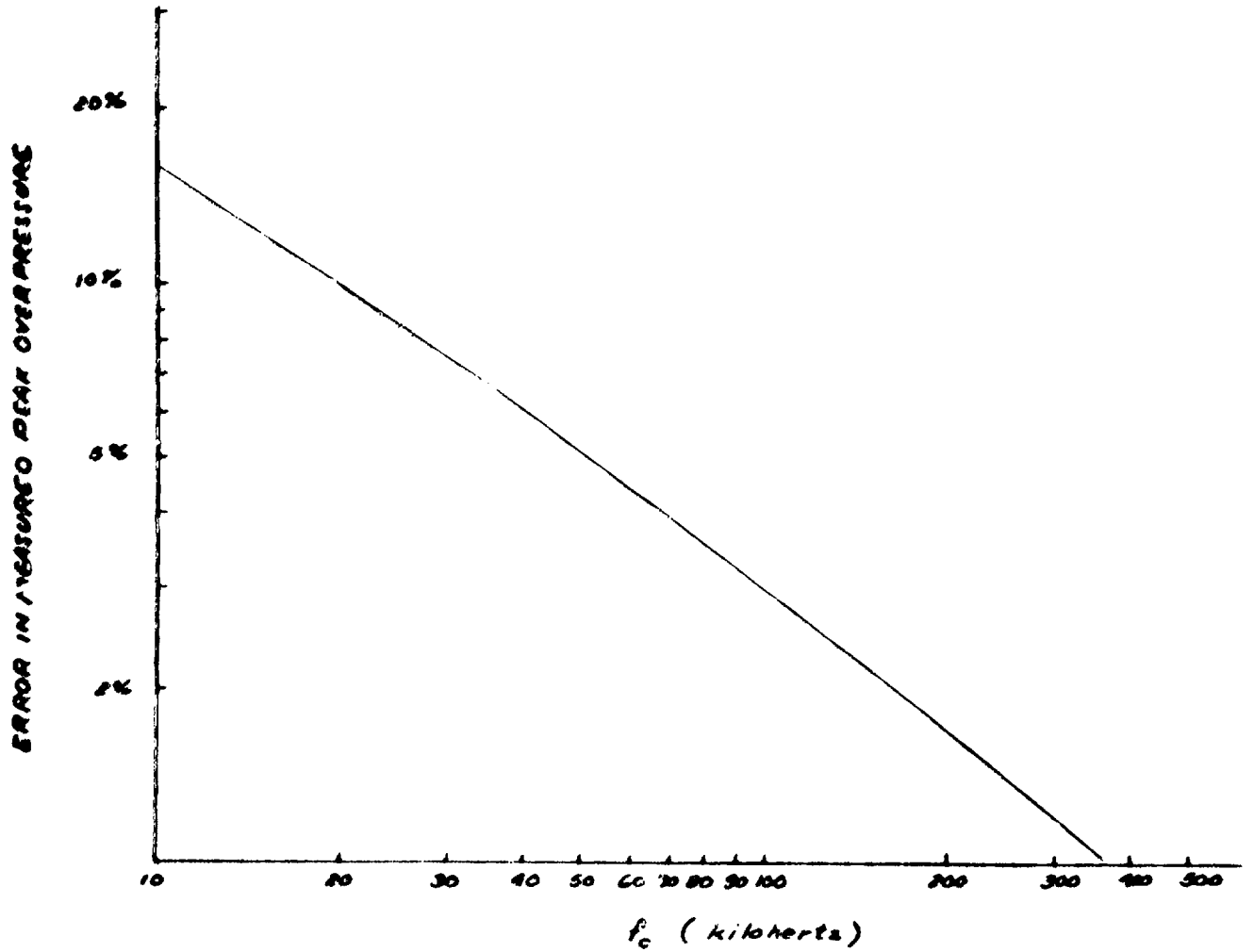

Figure A-3. Error in peak overpressure measurement 10,000 psi shock, 1 KT yield.

As $t \longrightarrow \infty$, $V_o \longrightarrow 0$ so

$$\int_0^\infty V_i \, dt = \int_0^\infty V_o \, dt$$

Therefore the total measured impulse equals the total impulse of the Brode profile, independent of frequency response and independent of any empirical corrections to the measured profile.

An alternate question is how close are the two impulses when t equals D, the duration of positive phase. In this case

$$\int_0^D V_i \, dt = \tau V_o \Big|_{t=D} + \int_0^D V_o \, dt$$

A short numerical calculation for f_c = 20 kHz shows

$$\tau V_o \Big|_{t=D} = 6.6 \times 10^{-10}$$

while

$$\int_c^e V_i \, dt = 12.5$$

So again the measured and input impulses are equal at the end of positive phase provided the bandwidth is 20 kHz or greater.

The last result can also be restated as follows: the impulses are equal at the end of positive phase provided V_i and V_o pass through zero simultaneously. Figure A2 shows that the measured response overshoots the Brode profile, settling down towards the profile at later times. If the frequency response is high enough, the measured pulse will catch up with the Brode profile at or before the duration of positive phase. The numbers of the preceding paragraph show that the frequency response required for the catchup is minimal.

Finally, it must be remembered that the results for measured impulse depend on the electrical analog chosen for the gage and recording system. More complex models would probably give different conclusions, at least in numerical detail. However, it does seem reasonable to assume that measured impulse is insensitive to frequency response.

DISTRIBUTION LIST

DEPARTMENT OF DEFENSE

Director
Defense Advanced Research Projects Agency
ATTN: NMRO
ATTN: PMO
ATTN: STO
ATTN: Technical Library

Defense Documentation Center
12 cy ATTN: TC

Director
Defense Nuclear Agency
ATTN: STSI, Archives
ATTN: DDST
2 cy ATTN: STTL, Tech. Library
2 cy ATTN: SPSS

Commander
Field Command
Defense Nuclear Agency
ATTN: FCPR
ATTN: FCT

Chief
Livermore Division Field Command, DNA
Lawrence Livermore Laboratory
ATTN: FCPRL

Weapons Systems Evaluation Group
ATTN: Document Control

DEPARTMENT OF THE ARMY

Dep. Chief of Staff for Rsch. Dev. & Acq.
Department of the Army
ATTN: Technical Library

Commander
Harry Diamond Laboratories
ATTN: AMXDO-TI, Tech. Lib.
ATTN: AMXDO-NP

Director
U.S. Army Ballistic Research Labs.
ATTN: J. H. Keefer, AMXBR-TL-IR
ATTN: Tech. Lib., Edward Baicy
ATTN: Julius J. Meszaros, AMXBR-X

Director
U.S. Army Engr. Waterways Exper. Sta.
ATTN: William Flathau
ATTN: Technical Library
ATTN: Guy Jackson
ATTN: John N. Strange
ATTN: Leo Ingram

Commander
U.S. Army Materiel [illegible] & Readiness Cmd.
ATTN: Technical Library

DEPARTMENT OF THE NAVY

Chief of Naval Research
Navy Department
ATTN: Technical Library

Officer-In-Charge
Civil Engineering Laboratory
ATTN: Technical Library
ATTN: R. J. O'Dello

Commander
Naval Facilities Engineering Command
ATTN: Technical Library

Commander
Naval Ship Engineering Center
ATTN: Technical Library

Commander
Naval Ship Rsch. and Development Ctr.
ATTN: Code L42-3, Library

Commander
Naval Ship Rsch. and Development Ctr.
Underwater Explosive Research Division
ATTN: Technical Library

Commander
Naval Surface Weapons Center
ATTN: Code WA501, Navy Nuc. Prgms. Off.
ATTN: Code WX21, Tech. Lib.
ATTN: Code 241, J. Petes

DEPARTMENT OF THE AIR FORCE

AF Geophysics Laboratory, AFSC
ATTN: SUOL AFCRL, Rsch. Lib.

AF Institute of Technology, AU
ATTN: Library AFIT, Bldg. 640, Area B

AF Weapons Laboratory, AFSC
ATTN: DEV, M. A. Plamondon
ATTN: SUL, Tech. Lib.
ATTN: DEX

HQ USAF/IN
ATTN: INATA

ENERGY RESEARCH & DEVELOPMENT ADMINISTRATION

University of California
Lawrence Livermore Laboratory
ATTN: Tech. Info., Dept. L-3

Sandia Laboratories
Livermore Laboratory
ATTN: Doc. Control for Tech. Library

ENERGY RESEARCH & DEVELOPMENT ADMINISTRATION (Continued)

Sandia Laboratories
ATTN: Doc. Con. for A. J. Chaban
ATTN: Doc. Con. for Org. 3422-1, Sandia Rpt. Coll.
ATTN: Doc. Con. for Luke J. Vortman

U.S. Energy Rsch. & Dev. Admin.
Albuquerque Operations Office
ATTN: Doc. Con. for Tech. Library

U.S. Energy Rsch. & Dev. Admin.
Division of Headquarters Services
ATTN: Doc. Con. for Class. Tech. Lib.

U.S. Energy Rsch. & Dev. Admin.
Nevada Operations Office
ATTN: Doc. Con. for Tech. Lib.

DEPARTMENT OF DEFENSE CONTRACTORS

Aerospace Corporation
ATTN: Prem N. Mathur
ATTN: Tech. Info. Services

Agbabian Associates
ATTN: M. Agbabian

Artec Associates Incorporated
ATTN: Stephen P. Gill
ATTN: Michael B. Gross

Civil/Nuclear Systems Corp.
ATTN: Robert Crawford

EG&G, Inc.
Albuquerque Division
ATTN: Technical Library

General Electric Company
TEMPO-Center for Advanced Studies
ATTN: DASIAC

IIT Research Institute
ATTN: Technical Library

Kaman Sciences Corporation
ATTN: Library
ATTN: Paul A. Ellis

Merritt Cases, Incorporated
ATTN: J. L. Merritt
ATTN: Technical Library

DEPARTMENT OF DEFENSE CONTRACTORS (Continued)

The Mitre Corporation
ATTN: Library

Nathan M. Newmark
Consulting Engineering Services
ATTN: Nathan M. Newmark

Physics International Company
ATTN: Doc. Con. for Charles Godfrey
ATTN: Doc. Con. for Fred M. Sauer
ATTN: Doc. Con. for Tech. Lib.
ATTN: Doc. Con. for Coye Vincent

R & D Associates
ATTN: J. G. Lewis
ATTN: Technical Library
ATTN: Bruce Hartenbaum

Science Applications, Inc.
ATTN: Technical Library
ATTN: Michael McKay

Science Applications, Inc.
ATTN: R. A. Shunk

Southwest Research Institute
ATTN: A. B. Wenzel
ATTN: Wilfred E. Baker

Stanford Research Institute
ATTN: Carl Peterson
ATTN: George R. Abrahamson
ATTN: Burt R. Gasten

Systems, Science and Software, Inc.
ATTN: Technical Library
ATTN: Donald R. Grine

TRW Systems Group
ATTN: Tech. Info. Center, S-1930

The Eric H. Wang
Civil Engineering Rsch. Fac.
ATTN: Larry Bickle
ATTN: Neal Baum

Weidlinger Assoc. Consulting Engineers
ATTN: Melvin L. Baron

Weidlinger Assoc. Consulting Engineers
ATTN: J. Isenberg